Hubbard band versus oxygen vacancy states in the correlated electron metal SrVO₃

S. Backes,[1] T. C. Rödel,[2,3] F. Fortuna,[2] E. Frantzeskakis,[2] P. Le Fèvre,[3] F. Bertran,[3] M. Kobayashi,[4] R. Yukawa,[4]
T. Mitsuhashi,[4] M. Kitamura,[4] K. Horiba,[4] H. Kumigashira,[4] R. Saint-Martin,[5] A. Fouchet,[6] B. Berini,[6] Y. Dumont,[6]
A. J. Kim,[1] F. Lechermann,[7,8] H. O. Jeschke,[1] M. J. Rozenberg,[9] R. Valentí,[1,*] and A. F. Santander-Syro[2,†]

[1]*Institut für Theoretische Physik, Goethe-Universität Frankfurt, Max-von-Laue-Strasse 1, 60438 Frankfurt am Main, Germany*
[2]*CSNSM, Univ. Paris-Sud, CNRS/IN2P3, Université Paris-Saclay, 91405 Orsay Cedex, France*
[3]*Synchrotron SOLEIL, L'Orme des Merisiers, Saint-Aubin-BP48, 91192 Gif-sur-Yvette, France*
[4]*Photon Factory, Institute of Materials Structure Science, High Energy Accelerator Research Organization (KEK),*
1-1 Oho, Tsukuba 305-0801, Japan
[5]*SP2M-ICMMO - UMR-CNRS 8182 Université Paris-Sud, Université Paris-Saclay, 91405 Orsay Cedex, France*
[6]*GEMaC, Université de Versailles St. Quentin en Y. - CNRS, Université Paris-Saclay, Versailles, France*
[7]*Institut für Theoretische Physik, Universität Hamburg, Jungiusstrasse 9, 20355 Hamburg, Germany*
[8]*Institut für Keramische Hochleistungswerkstoffe, TU Hamburg-Harburg, D-21073 Hamburg, Germany*
[9]*Laboratoire de Physique des Solides, CNRS, Univ. Paris-Sud, Université Paris-Saclay, 91405 Orsay Cedex, France*

We study the effect of oxygen vacancies on the electronic structure of the model strongly correlated metal SrVO₃. By means of angle-resolved photoemission spectroscopy (ARPES) synchrotron experiments, we investigate the systematic effect of the UV dose on the measured spectra. We observe the onset of a spurious dose-dependent prominent peak at an energy range where the lower Hubbard band has been previously reported in this compound, raising questions on its previous interpretation. By a careful analysis of the dose-dependent effects we succeed in disentangling the contributions coming from the oxygen vacancy states and from the lower Hubbard band. We obtain the ARPES spectrum in the limit of a negligible concentration of vacancies, where a clear signal of a lower Hubbard band remains. We support our study by means of state-of-the-art *ab initio* calculations that include correlation effects and the presence of oxygen vacancies. Our results underscore the relevance of potential spurious states affecting ARPES experiments in correlated metals, which are associated with the ubiquitous oxygen vacancies as extensively reported in the context of a two-dimensional electron gas at the surface of insulating d^0 transition metal oxides.

DOI: 10.1103/PhysRevB.94.241110

Introduction. A major challenge of modern physics is to understand the fascinating phenomena in strongly correlated transition metal oxides (TMOs), which emerge in the neighborhood of the Mott insulator state. Some preeminent examples that have gathered interest for almost 30 years are high temperature superconductivity, colossal magnetoresistance, heavy fermion physics, and, of course, the Mott metal-insulator transition itself [1]. Significant theoretical progress was made with the introduction of dynamical mean field theory (DMFT) and its combination with *ab initio* density functional methods [local density approximation (LDA)+DMFT], which allows treatment of the interactions promoting itinerancy and localization of electrons on equal footing [2–4]. Among the most emblematic achievements of DMFT is the prediction of a Hubbard satellite, which separates from the conduction band of a metal. This satellite results from the partial localization of conduction electrons due to their mutual Coulomb repulsion. Early DMFT studies also showed that it is the precursor of the localized electronic states of a Mott insulator [5]. Since then, these predictions promoted a large number of studies using photoemission spectroscopy, which is a technique to directly probe the presence of Hubbard bands. In this context, the TMO system SrVO₃ has emerged as the *drosophila* model system to test the predictions of strongly correlated electron

theories. In fact, SrVO₃ is arguably the simplest correlated metal. It is a simple cubic perovskite, with nominally one electron per V site, which occupies a threefold degenerate t_{2g} conduction band. While the presence of a satellite in the photoemission spectra of Ni metal was already well known, in the context of correlated TMOs, the Hubbard band was originally reported in a systematic investigation of Ca$_{1-x}$Sr$_x$VO₃ [6], which was followed by many subsequent studies, including angle-resolved photoemission spectroscopy (ARPES) [7–9] and comparisons with theoretical predictions (see, for instance, Refs. [10–20], among others).

One of the most salient features in SrVO₃ is the observation of a broad peak at an energy of about −1.5 eV in angle integrated photoemission spectra (upper black curve in Fig. 1), which is interpreted as a Hubbard satellite linked to the V t_{2g} electrons. This feature is also seen in a large range of $3d^1$ materials [21,22]. The ratio of spectral strength between the quasiparticle (QP) state and the incoherent satellite in SrVO₃ is an important indicator of the magnitude of electron correlations [1,2]. However, photoemission experiments using different photon energies or light brilliance have reported very dissimilar values for such a ratio [11], making the quantitative benchmarking of realistic *ab initio* theories for correlated electron systems difficult [6,11,18,23,24]. Moreover, as shown in Fig. 1, a broad peak at about the same energy is also observed in several d^0 TMO cubic perovskites, such as SrTiO₃, KTaO₃, or anatase TiO₂. Nevertheless, in all these cases the feature has been clearly linked to the presence of oxygen

*valenti@itp.uni-frankfurt.de
†andres.santander@csnsm.in2p3.fr
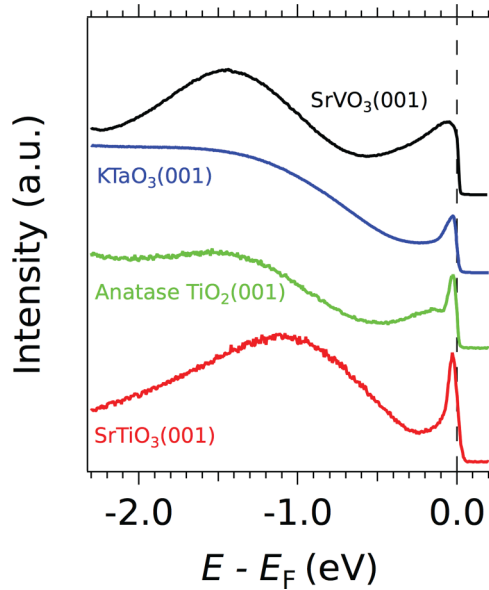
FIG. 1. Integrated UV photoemission spectra for various perovskite oxides, showing a quasiparticle peak at E_F and an in-gap state at energies between 1 and 1.5 eV. For SrVO$_3$ (upper black curve), a correlated-electron metal, the QP peak corresponds to the bulk conduction band, and as will be shown further, the in-gap state is a superposition of the lower Hubbard band and localized electronic states associated with oxygen vacancies. For the other d^0 oxides, such as KTaO$_3$ (blue curve), anatase TiO$_2$ (green curve), or SrTiO$_3$ (red curve), the QP peak and in-gap state correspond respectively to a confined quasi-2D electron gas at the sample surface and to localized states, all formed by oxygen vacancies. The crystal orientation (normal to the samples' surface) is indicated in all cases.

defects [25–32]. Interestingly, recent *ab initio* calculations show that the spectral weight at -1.3 eV in SrTiO$_3$ most likely is not of Ti t_{2g} orbital character, but should be understood as an in-gap defect state with Ti e_g character [33–36]. Thus, we are confronted with the fact that at about 1.5 eV below the Fermi level (E_F), we find the lower Hubbard bands of d^1 systems as well as the in-gap states of oxygen-deficient d^0 systems. In view of these observations one may unavoidably wonder (and worry), despite the great success of DMFT methods, whether the putative Hubbard satellite of SrVO$_3$ might also originate from oxygen vacancy states. Moreover, one should also worry about the possibility of these extrinsic states affecting the features of the conduction band dispersion.

In the present Rapid Communication we resolve these issues in a thorough manner. We present a systematic photoemission study of SrVO$_3$, to demonstrate dramatic consequences in the spectra due to the creation of oxygen vacancies. Using ARPES, we directly show that the UV or x-rays used for measurements can produce a large enhancement, of almost an order of magnitude, of the peak at -1.5 eV, similar to the effect observed in d^0 oxide insulators [25–28,37]. Despite these significant effects on the energy states around the Mott-Hubbard band, we are able to determine the bulk SrVO$_3$ photoemission spectrum in the limit of a negligible concentration of vacancies, where a clear signal of the dispersive correlated Hubbard band remains. We support the interpretation of the experimental data by means

of state-of-the-art LDA+DMFT calculations on SrVO$_3$ *with oxygen vacancies*. Consistent with our experimental data, the calculations show that oxygen vacancies produce states (of e_g symmetry) at energies near the Hubbard satellite. While our study provides definite evidence of a correlated Hubbard band in SrVO$_3$ as predicted by DMFT, it also underlines the significant effects due to oxygen vacancies, which may also affect photoemission data in other TMOs.

Methods. The bulk-like relaxed, crystalline (001) oriented SrVO$_3$ thin films were grown by pulsed laser deposition (PLD) either at the GEMaC laboratory, then measured at the CASSIOPEE beamline of Synchrotron SOLEIL, or in a PLD chamber directly connected to the ARPES setup at beamline 2A of KEK-Photon Factory (KEK-PF) [9,38,39]. To clean the surfaces in UHV prior to ARPES experiments at SOLEIL, the SrVO$_3$ thin films were annealed at $550\,^{\circ}$C for $t = 5$–20 min at pressures lower than 2×10^{-8} Torr. At KEK-PF, the PLD growth was performed under a pressure below 10^{-7} Torr, to obtain UHV-clean surfaces, using a Sr$_2$V$_2$O$_7$ target, which has excess oxygen with respect to SrVO$_3$, thus minimizing the formation of vacancies during the growth. In all cases, the surface quality was confirmed right before ARPES measurements by low-energy electron diffraction (LEED). The thin films measured at KEK-PF showed a $c(4 \times 4)$ surface reconstruction, which does not affect the analysis and conclusions of this work. For the ARPES measurements we used linearly polarized photons in the energy range 30–110 eV and hemispherical electron analyzers with vertical slits at SOLEIL and horizontal slits at KEK-PF. The angular and energy resolutions were 0.25° and 15 meV. The mean diameter of the incident photon beam was smaller than $100\,\mu$m. The UV light brilliance, measured using calibrated photodiodes, was $\approx 5 \times 10^9$ photons s^{-1} μm^{-2} at SOLEIL, and about 100 times smaller at KEK-PF. The samples were cooled down to $T = 20$ K before measuring. Unless specified otherwise, all data were taken at that temperature. The results were reproduced on more than five samples. All through this Rapid Communication, directions and planes are defined in the cubic unit cell of SrVO$_3$. We denote $[hkl]$ the crystallographic directions in real space, $\langle hkl \rangle$ the corresponding directions in reciprocal space, and (hkl) the planes orthogonal to those directions. The indices h, k, and l of Γ_{hkl} correspond to the reciprocal lattice vectors of the cubic unit cell of SrVO$_3$. The Supplemental Material [40] presents further details about the sample growth and measurements.

Experimental results. Figure 2(a) shows the integrated photoemission spectra of SrVO$_3$ as a function of the UV dose, measured at CASSIOPEE SOLEIL under the same conditions of light brilliance of any standard ARPES experiment at a third-generation synchrotron. The measurements were done by continuously irradiating the sample with $h\nu = 33$ eV photons while recording the spectra as a function of irradiation time, with an accumulation time of about 2 min per spectrum. The blue and black curves show spectra for the lowest and highest measured doses, obtained respectively after ~ 2 min and ~ 2 h of irradiation. These data clearly demonstrate that the very UV or x-rays used for photoemission experiments can produce radical changes in the measured spectra of SrVO$_3$. Note in fact that a similar effect has been observed for VO$_2$ [41]. In particular, from Fig. 2(a) we observe that the amplitude of
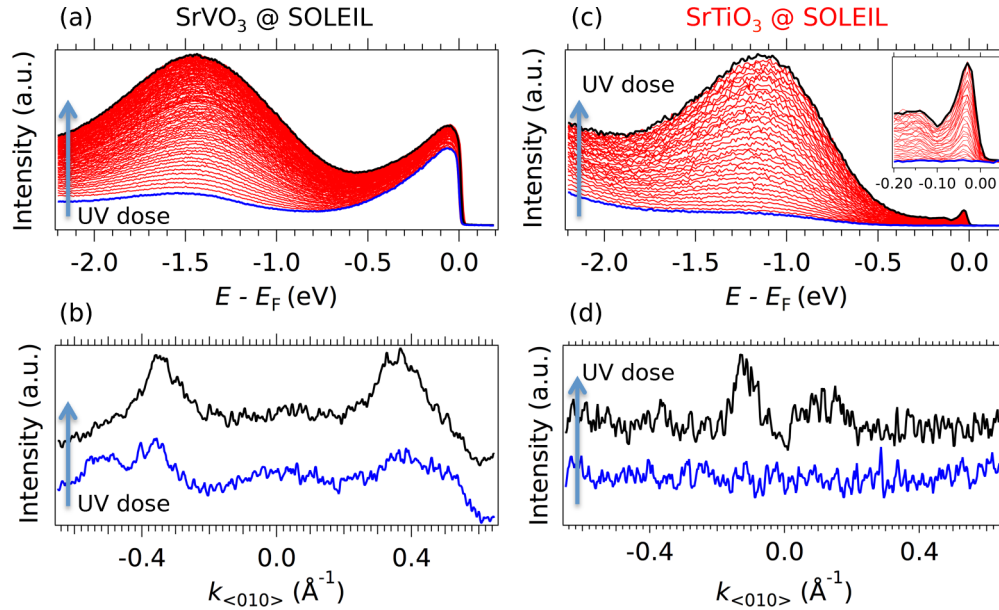
FIG. 2. (a) Photoemission spectra of $SrVO_3$ as a function of UV dose, measured at Synchrotron SOLEIL ($h\nu = 33$ eV). The energy distribution curves (EDCs) were extracted from raw ARPES data around the Γ_{002} point integrated along the $k = \langle 010 \rangle$ direction. (b) Corresponding momentum distribution curves (MDCs) integrated over 50 meV below E_F. Peaks in the MDCs indicate the Fermi momenta. (c), (d) Same as (a), (b) for $SrTiO_3$ ($h\nu = 47$ eV). The filling of a 2DEG upon UV irradiation is evidenced by the formation of QP peaks in the EDCs and MDCs at E_F [inset of (c) and (d), respectively]. All data were taken at 20 K.

the in-gap state at -1.5 eV, and, more significantly, the ratio of in-gap to quasiparticle (QP) amplitudes, strongly increase with increasing UV dose, going from about $1 : 3$ in a pristine sample to more than $2 : 1$ in a heavily irradiated sample. Importantly, note that the QP peak position remains basically dose independent, implying that the carriers created by the UV or x irradiation do not significantly dope the conduction band, and form dominantly localized states. This is confirmed in Fig. 2(b), which shows that the Fermi momenta of the QP band, given by the peak positions in the momentum distribution curves (MDCs) at E_F, are also dose independent. Additional data presented in the Supplemental Material further demonstrate that our measurements yield the expected 3D bulk Fermi surface of $SrVO_3$. Thus, the observed increase in intensity of the in-gap state upon UV irradiation *cannot* be ascribed to a change in filling of the conduction band, which could have affected the electron correlations. Instead, this unambiguously shows the light-assisted formation of localized defect states at essentially the same energy as that of the expected intrinsic lower Hubbard band—which should then resemble the in-gap peak observed at the lowest UV doses.

In fact, as mentioned previously, it is well established that strong doses of UV or x-rays create a large concentration of oxygen vacancies in several d^0 perovskites [25–32,42]. As illustrated in Figs. 2(c) and 2(d) for the case of $SrTiO_3$, the progressive doping of the surface region with oxygen vacancies, due to synchrotron UV irradiation, has two effects: the formation of a very intense in-gap state at about -1.3 eV, and, in contrast to $SrVO_3$, the simultaneous creation of a sharp QP peak at E_F corresponding to a confined quasi-2D electron gas (2DEG) at the samples' surface. The effective mass of such 2DEG, precisely determined by ARPES, matches the mass expected from density functional theory calcula-

tions [25,26,43,44]. Thus, as in $SrVO_3$, the increase in intensity of the in-gap state observed in $SrTiO_3$ upon UV or x irradiation cannot be due to an onset or increase of electron correlations, and should be ascribed to an extrinsic effect.

We therefore conclude that, in $SrVO_3$, exposure to synchrotron UV or x-rays creates oxygen vacancies, which are in turn responsible for the extrinsic increase in intensity of the in-gap state evidenced by our measurements. This effect can seriously obscure the determination of the spectral function of this model system, thus hampering the advancement of valid theories for correlated electron systems.

The findings described above imply that the correct experimental determination of the vacancy-free photoemission spectrum of $SrVO_3$ should (i) use samples that from the beginning have the lowest possible concentration of oxygen vacancies, and (ii) use doses of UV or x-ray light low enough to avoid light-induced changes in the measured spectra. To this end, we measured $SrVO_3$ thin films grown directly *in situ* at beamline 2A of KEK-PF. As mentioned before, the growth protocol of such thin films minimizes the formation of vacancies, while the UV light brilliance at KEK-PF is $\sim$100 times smaller than the one in Figs. 2(a) and 2(b) from measurements at SOLEIL. We checked (see the Supplemental Material) that under these conditions the spectra did not change with time, even after several hours of measurements. The resulting energy-momentum ARPES map, and its second derivative, are presented in Figs. 3(a) and 3(b). One clearly observes the dispersing QP band along with an also dispersive in-gap state of weaker intensity, corresponding to the intrinsic lower Hubbard band, as reported in previous works [7]. The intrinsic spectral function of $SrVO_3$ will then be given by such a photoemission spectrum, which approaches the vacancy-free limit, modulo dipole-transition matrix elements, inherent to
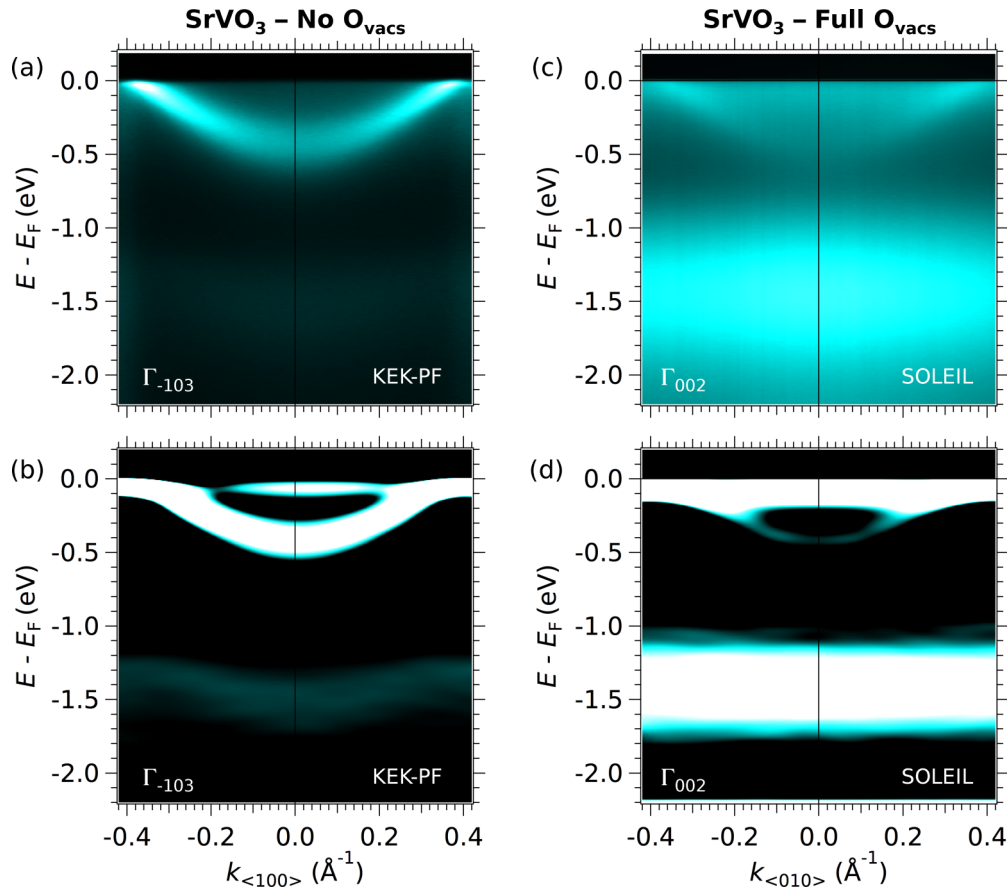
FIG. 3. (a) Energy-momentum ARPES intensity map measured at KEK-PF with a low UV dose on a $SrVO_3$ sample prepared *in situ*, using a well-established protocol to minimize the formation of oxygen vacancies (see the main text and Supplemental Material). Note that due to the choice of light polarization, the heavy bands along (100) are not observed and only the contribution of the light d_{xy} band is detected. The data were acquired at $h\nu = 88$ eV around $\Gamma_{\bar{1}03}$. (b) Second derivative (negative values) of the map in (a). The use of second derivatives allows a better visualization of the dispersion of both the quasiparticle and Mott-Hubbard bands on the same color plot. The dispersionless feature at E_F is a spurious effect of such a second derivative on the Fermi-Dirac cutoff. (c), (d) Same as (a), (b) after a strong UV irradiation dose, measured at SOLEIL ($h\nu = 33$ eV), typical of modern third-generation synchrotrons. The measurements were done at $h\nu = 33$ eV close to Γ_{002}. All data were taken at 20 K. Note that at constant photon energy, ARPES maps out the electronic structure at a spherical surface of three-dimensional (3D) k space, which can be locally approximated to a plane for all our measurements (details in the Supplemental Material). The different choice of photon energies and k-space positions for measurements at KEK-PF [(a) and (b)] and SOLEIL [(c) and (d)] was dictated by the different geometrical configurations and constraints of the beamlines in both synchrotrons.

the photoemission process, which can still modulate the intensity of the QP peak relative to the Hubbard peak. A calculation of such matrix elements requires a full one-step calculation of the photoemission process, which is beyond the scope of this work. By contrast, Figs. 3(c) and 3(d) show the momentum-resolved electronic structure of a sample, measured at SOLEIL, that was intensively irradiated. There, the peak at -1.5 eV becomes broader, more intense, and nondispersive—all characteristic signatures of a high random concentration of oxygen vacancies.

Numerical calculations. To rationalize from a microscopic point of view the influence of oxygen vacancies on the electronic structure of $SrVO_3$, we performed charge self-consistent LDA+DMFT calculations for bulk $SrVO_3$ and various relaxed oxygen-deficient $SrVO_3$ supercells. The latter are computationally demanding calculations. We shall focus here on the case of a $2 \times 2 \times 3$ supercell with two oxygen vacancies located at opposite apical sites of one vanadium atom, as shown

in the inset of Fig. 4(b). We use such a vacancy arrangement as it is the prototypical one for d^0 compounds [43].

For our LDA+DMFT calculations we chose values of $U = 2.5$ eV and $J = 0.6$ eV for vanadium and included the effects of bandwidth renormalization due to dynamically screened Coulomb interactions by following the prescription suggested in Ref. [45] (the LDA+DMFT unrenormalized data are shown in the Supplemental Material). In Figs. 4(a) and 4(c) we show, respectively, the results of the k-integrated and k-resolved spectral functions for bulk $SrVO_3$ without oxygen vacancies. We find the expected features of a t_{2g} quasiparticle peak at the Fermi level and a lower Hubbard band at negative energies of the same t_{2g} nature, in agreement with the photoemission spectra in Fig. 2(a) and Figs. 3(a) and 3(b). The light band at E_F along $k_{\langle 100 \rangle}$ [Fig. 4(c)] consists of two degenerate bands of d_{xy} and d_{xz} characters, while the heavy band along the same direction has d_{yz} character. While comparing with the measured k-resolved spectral function [Figs. 3(a) and 3(b)],
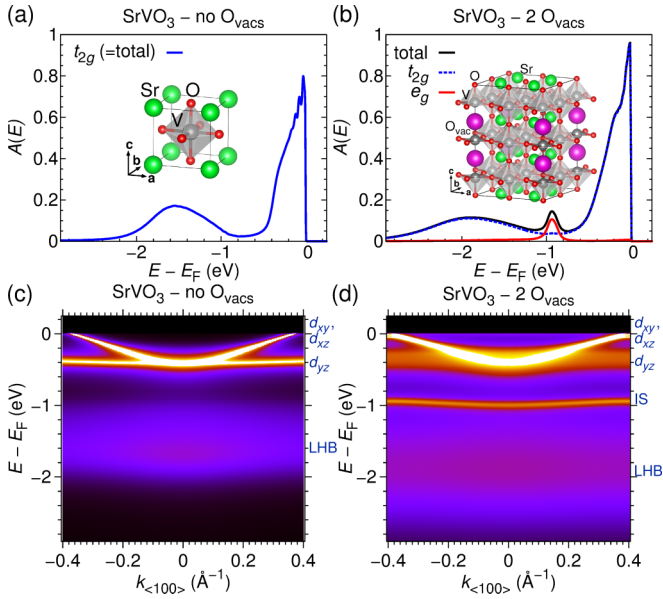
FIG. 4. LDA+DMFT results for SrVO$_3$ including bandwidth renormalization effects [45]. (a) k-integrated spectral function for bulk SrVO$_3$. The V t_{2g} orbitals show a quasiparticle peak at E_F and a lower Hubbard band at -1.6 eV. (b) Spectral function for the $2 \times 2 \times 3$ supercell of SrVO$_3$ with two oxygen vacancies. An additional nondispersive V e_g vacancy state originating from the V atom neighboring the oxygen vacancies leads to a sharp peak below the Fermi level at ~ -1.0 eV. The V t_{2g} orbitals show a quasiparticle peak at E_F and a lower Hubbard band at -1.8 eV. (c) and (d) show the corresponding spectral functions (multiplied by a Fermi-Dirac function at 20 K) along the X-Γ-X path.

one should bear in mind that along Γ-X (or Γ-Y) the heavy d_{yz} (or d_{xz}) bands are silenced by dipole-transition selection rules in the experiment [25]. Inclusion of bandwidth renormalization [45] renders the lower Hubbard band at an energy (-1.6 eV) in reasonable agreement with experiment (-1.5 eV). We adopted typical values for U and J from the literature. We did not attempt to further optimize the values to get a better quantitative agreement with the experimental data, for two reasons: First is the heavy numerical cost, and second, as we show next in the calculations with oxygen vacancies, the adopted values facilitate the distinct visualization of the contributions from the Hubbard and localized states to the incoherent peak at ~ -1.5 eV.

The removal of oxygen atoms in the system leads to the donation of two electrons per oxygen to its surrounding. Already at the level of density functional theory (DFT) in the local density approximation (LDA) (see the Supplemental Material), we find that most of the charge coming from the additional electrons is transferred to the $3d_{z^2}$ orbitals of the neighboring V atom, developing into a sharp peak of e_g symmetry located around -1.0 eV, i.e., at an energy close to the

position of the experimentally observed oxygen vacancy states. In analogy to the experimental average over many lattice sites, note that averaging among various supercells with different oxygen vacancy locations and concentrations (which is beyond the scope of the present work) would result in a wider in-gap e_g band, as demonstrated for the case of SrTiO$_3$ (see Fig. 3 of Ref. [34]) and for some cases in SrVO$_3$ (see the Supplemental Material, Fig. S7). By including electronic correlations within (bandwidth renormalized) LDA+DMFT we then see that all the experimental observations qualitatively emerge. In fact, the conducting t_{2g} orbitals develop a lower Hubbard band peaked at energies about -1.8 eV [Figs. 4(b) and 4(d)], similar to the bulk case without oxygen vacancies. Most notably, this lower Hubbard satellite does not increase in amplitude with the introduction of vacancies, but rather broadens. In addition, the oxygen vacancy defect states situated at about -1 eV remain qualitatively unchanged by the correlation effects, but experience a broadening with respect to the pure LDA case. This is in agreement with the photoemission data, evidencing that the increase in intensity of the in-gap state in the oxygen-deficient SrVO$_3$ is not to be attributed to an increase in population of the lower Hubbard satellite, but instead to the manifestation of vacancy states of e_g character.

Conclusions. In summary, we performed a detailed study of the effects of oxygen vacancies in the spectroscopy of the archetypal strongly correlated electron system SrVO$_3$. We found that oxygen vacancy states, which are created by UV or x-ray irradiation, occur at energies close to the Hubbard satellite. This dramatically affects the measured line shape of the Mott-Hubbard band and the ratio of intensities between the quasiparticle and the Mott-Hubbard peaks. By means of a systematic study under a controlled irradiation dose, using samples directly grown *in situ*, we were able to obtain the photoemission spectrum of the bulk SrVO$_3$ system in the limit of a negligible concentration of oxygen vacancies. Our experimental interpretation is supported by LDA+DMFT calculations, which provided further insight into the likely nature of the oxygen vacancy states.

[1] M. Imada, A. Fujimori, and Y. Tokura, Metal-insulator transitions, Rev. Mod. Phys. **70**, 1039 (1998).

[2] A. Georges, G. Kotliar, W. Krauth, and M. J. Rozenberg, Dynamical mean field theory of strongly correlated electrons

and the limit of infinite dimensions, Rev. Mod. Phys. **68**, 13 (1996).

[3] G. Kotliar and D. Vollhardt, Strongly correlated materials: Insights from dynamical mean-field theory, Phys. Today **57**(3), 53 (2004).

[4] G. Kotliar, S. Y. Savrasov, K. Haule, V. S. Oudovenko, O. Parcollet, and C. A. Marianetti, Electronic structure calculations with dynamical mean-field theory, Rev. Mod. Phys. **78**, 865 (2006).

[5] X. Y. Zhang, M. J. Rozenberg, and G. Kotliar, Mott Transition in the $d = \infty$ Hubbard Model at Zero Temperature, Phys. Rev. Lett. **70**, 1666 (1993).

[6] I. H. Inoue, I. Hase, Y. Aiura, A. Fujimori, Y. Haruyama, T. Maruyama, and Y. Nishihara, Systematic Development of the Spectral Function in the $3d^1$ Mott-Hubbard System $Ca_{1-x}Sr_xVO_3$, Phys. Rev. Lett. **74**, 2539 (1995).

[7] M. Takizawa, M. Minohara, H. Kumigashira, D. Toyota, M. Oshima, H. Wadati, T. Yoshida, A. Fujimori, M. Lippmaa, M. Kawasaki, H. Koinuma, G. Sordi, and M. Rozenberg, Coherent and incoherent d band dispersions in $SrVO_3$, Phys. Rev. B **80**, 235104 (2009).

[8] T. Yoshida, M. Hashimoto, T. Takizawa, A. Fujimori, M. Kubota, K. Ono, and H. Eisaki, Mass renormalization in the bandwidth-controlled Mott-Hubbard systems $SrVO_3$ and $CaVO_3$ studied by angle-resolved photoemission spectroscopy, Phys. Rev. B **82**, 085119 (2010).

[9] S. Aizaki, T. Yoshida, K. Yoshimatsu, M. Takizawa, M. Minohara, S. Ideta, A. Fujimori, K. Gupta, P. Mahadevan, K. Horiba, H. Kumigashira, and M. Oshima, Self-Energy on the Low- to High-Energy Electronic Structure of Correlated Metal $SrVO_3$, Phys. Rev. Lett. **109**, 056401 (2012).

[10] M. J. Rozenberg, I. Inoue, H. Makino, F. Iga, and Y. Nishihara, Low Frequency Spectroscopy of the Correlated Metallic System $Ca_{1-x}Sr_xVO_3$, Phys. Rev. Lett. **76**, 4781 (1996).

[11] A. Sekiyama, H. Fujiwara, S. Imada, S. Suga, H. Eisaki, S. I. Uchida, K. Takegahara, H. Harima, Y. Saitoh, I. A. Nekrasov, G. Keller, D. E. Kondakov, A. V. Kozhevnikov, Th. Pruschke, K. Held, D. Vollhardt, and V. I. Anisimov, Mutual Experimental and Theoretical Validation of Bulk Photoemission Spectra of $Sr_{1-x}Ca_xVO_3$, Phys. Rev. Lett. **93**, 156402 (2004).

[12] E. Pavarini, S. Biermann, A. Poteryaev, A. I. Lichtenstein, A. Georges, and O. K. Andersen, Mott Transition and Suppression of Orbital Fluctuations in Orthorhombic $3d^1$ Perovskites, Phys. Rev. Lett. **92**, 176403 (2004).

[13] B. Amadon, F. Lechermann, A. Georges, F. Jollet, T. O. Wehling, and A. I. Lichtenstein, Plane-wave based electronic structure calculations for correlated materials using dynamical mean-field theory and projected local orbitals, Phys. Rev. B **77**, 205112 (2008).

[14] M. Aichhorn, L. Pourovskii, V. Vildosola, M. Ferrero, O. Parcollet, T. Miyake, A. Georges, and S. Biermann, Dynamical mean-field theory within an augmented plane-wave framework: Assessing electronic correlations in the iron pnictide LaFeAsO, Phys. Rev. B **80**, 085101 (2009).

[15] M. Karolak, T. O. Wehling, F. Lechermann, and A. I. Lichtenstein, General DFT++ method implemented with projector augmented waves: Electronic structure of $SrVO_3$ and the Mott transition in $Ca_{2-x}Sr_xRuO_4$, J. Phys.: Condens. Matter **23**, 085601 (2011).

[16] H. Lee, K. Foyevtsova, J. Ferber, M. Aichhorn, H. O. Jeschke, and R. Valentí, Dynamical cluster approximation within an augmented plane wave framework: Spectral properties of $SrVO_3$, Phys. Rev. B **85**, 165103 (2012).

[17] J. M. Tomczak, M. Casula, T. Miyake, F. Aryasetiawan, and S. Biermann, Combined GW and dynamical mean-field theory: Dynamical screening effects in transition metal oxides, Europhys. Lett. **100**, 67001 (2012).

[18] C. Taranto, M. Kaltak, N. Parragh, G. Sangiovanni, G. Kresse, A. Toschi, and K. Held, Comparing quasiparticle GW+DMFT and LDA+DMFT for the test bed material $SrVO_3$, Phys. Rev. B **88**, 165119 (2013).

[19] J. M. Tomczak, M. Casula, T. Miyake, and S. Biermann, Asymmetry in band widening and quasiparticle lifetimes in $SrVO_3$: Competition between screened exchange and local correlations from combined GW and dynamical mean-field theory GW+DMFT, Phys. Rev. B **90**, 165138 (2014).

[20] A. van Roekeghem and S. Biermann, Screened exchange dynamical mean field theory and its relation to density functional theory: $SrVO_3$ and $SrTiO_3$, Europhys. Lett. **108**, 57003 (2014).

[21] A. Fujimori, I. Hase, H. Namatame, Y. Fujishima, Y. Tokura, H. Eisaki, S. Uchida, K. Takegahara, and F. M. F. de Groot, Evolution of the Spectral Function in Mott-Hubbard Systems with d^1 Configuration, Phys. Rev. Lett. **69**, 1796 (1992).

[22] K. Morikawa, T. Mizokawa, A. Fujimori, Y. Taguchi, and Y. Tokura, Photoemission spectral weight distribution in $Y_{1-x}Ca_xTiO_3$, Phys. Rev. B **54**, 8446 (1996).

[23] I. A. Nekrasov, G. Keller, D. E. Kondakov, A. V. Kozhevnikov, Th. Pruschke, K. Held, D. Vollhardt, and V. I. Anisimov, Comparative study of correlation effects in $CaVO_3$ and $SrVO_3$, Phys. Rev. B **72**, 155106 (2005).

[24] R. Eguchi, T. Kiss, S. Tsuda, T. Shimojima, T. Mizokami, T. Yokoya, A. Chainani, S. Shin, I. H. Inoue, T. Togashi, S. Watanabe, C. Q. Zhang, C. T. Chen, M. Arita, K. Shimada, H. Namatame, and M. Taniguchi, Bulk- and Surface-Sensitive High-Resolution Photoemission Study of Two Mott-Hubbard Systems: $SrVO_3$ and $CaVO_3$, Phys. Rev. Lett. **96**, 076402 (2006).

[25] A. F. Santander-Syro, O. Copie, T. Kondo, F. Fortuna, S. Pailhès, R. Weht, X. G. Qiu, F. Bertran, A. Nicolaou, A. Taleb-Ibrahimi, P. Le Fèvre, G. Herranz, M. Bibes, N. Reyren, Y. Apertet, P. Lecoeur, A. Barthélémy, and M. J. Rozenberg, Two-dimensional electron gas with universal subbands at the surface of $SrTiO_3$, Nature (London) **469**, 189 (2011).

[26] W. Meevasana, P. D. C. King, R. H. He, S.-K. Mo, M. Hashimoto, A. Tamai, P. Songsiriritthigul, F. Baumberger, and Z.-X. Shen, Creation and control of a two-dimensional electron liquid at the bare $SrTiO_3$ surface, Nat. Mater. **10**, 114 (2011).

[27] P. D. C. King, R. H. He, T. Eknapakul, P. Buaphet, S.-K. Mo, Y. Kaneko, S. Harashima, Y. Hikita, M. S. Bahramy, C. Bell, Z. Hussain, Y. Tokura, Z.-X. Shen, H. Y. Hwang, F. Baumberger, and W. Meevasana, Subband Structure of a Two-Dimensional Electron Gas Formed at the Polar Surface of the Strong Spin-Orbit Perovskite $KTaO_3$, Phys. Rev. Lett. **108**, 117602 (2012).

[28] T. C. Rödel, F. Fortuna, F. Bertran, M. Gabay, M. J. Rozenberg, A. F. Santander-Syro, and P. Le Fèvre, Engineering of two-dimensional electron gases at the (001) and (101) surfaces of TiO_2 anatase using light, Phys. Rev. B **92**, 041106(R) (2015).

[29] S. Moser, L. Moreschini, J. Jaćimović, O. S. Barišić, H. Berger, A. Magrez, Y. J. Chang, K. S. Kim, A. Bostwick, E. Rotenberg, L. Forró, and M. Grioni, Tunable Polaronic Conduction in Anatase TiO_2, Phys. Rev. Lett. **110**, 196403 (2013).

[30] Y. Aiura, I. Hase, H. Bando, T. Yasue, T. Saitoh, and D. S. Dessau, Photoemission study of the metallic state of lightly electron-doped $SrTiO_3$, Surf. Sci. **515**, 61 (2002).

[31] S. McKeown Walker, A. de la Torre, F. Y. Bruno, A. Tamai, T. K. Kim, M. Hoesch, M. Shi, M. S. Bahramy, P. D. C. King, and F. Baumberger, Control of a Two-Dimensional Electron Gas on $SrTiO_3$(111) by Atomic Oxygen, Phys. Rev. Lett. **113**, 177601 (2014).

[32] S. McKeown Walker, F. Y. Bruno, Z. Wang, A. de la Torre, S. Riccó, A. Tamai, T. K. Kim, M. Hoesch, M. Shi, M. S. Bahramy, P. D. C. King, and F. Baumberger, Carrier-density control of the $SrTiO_3$(001) surface 2D electron gas studied by ARPES, Adv. Mater. **27**, 3894 (2015).

[33] C. Lin, C. Mitra, and A. A. Demkov, Orbital ordering under reduced symmetry in transition metal perovskites: Oxygen vacancy in $SrTiO_3$, Phys. Rev. B **86**, 161102(R) (2012).

[34] H. O. Jeschke, J. Shen, and R. Valentí, Localized versus itinerant states created by multiple oxygen vacancies in $SrTiO_3$, New J. Phys. **17**, 023034 (2015).

[35] M. Altmeyer, H. O. Jeschke, O. Hijano-Cubelos, C. Martins, F. Lechermann, K. Koepernik, A. Santander-Syro, M. J. Rozenberg, R. Valentí, and M. Gabay, Magnetism, Spin Texture and In-Gap States: Atomic Specialization at the Surface of Oxygen-Deficient $SrTiO_3$, Phys. Rev. Lett. **116**, 157203 (2016).

[36] F. Lechermann, L. Boehnke, D. Grieger, and C. Piefke, Electron correlation and magnetism at the $LaAlO_3/SrTiO_3$ interface: A DFT+DMFT investigation, Phys. Rev. B **90**, 085125 (2014).

[37] A. F. Santander-Syro, C. Bareille, F. Fortuna, O. Copie, M. Gabay, F. Bertran, A. Taleb-Ibrahimi, P. Le Fèvre, G. Herranz, N. Reyren, M. Bibes, A. Barthélémy, P. Lecoeur, J. Guevara, and M. J. Rozenberg, Orbital symmetry reconstruction and strong mass renormalization in the two-dimensional electron gas at the surface of $KTaO_3$, Phys. Rev. B **86**, 121107(R) (2012).

[38] K. Yoshimatsu, T. Okabe, H. Kumigashira, S. Okamoto, S. Aizaki, A. Fujimori, and M. Oshima, Dimensional-Crossover-Driven Metal-Insulator Transition in $SrVO_3$ Ultrathin Films, Phys. Rev. Lett. **104**, 147601 (2010).

[39] A. Fouchet, M. Allain, B. Bérini, E. Popova, P.-E. Janolin, N. Guiblin, E. Chikoidze, J. Scola, D. Hrabovsky, Y. Dumont, and N. Keller, Study of the electronic phase transition with low dimensionality in $SrVO_3$ thin films, Mater. Sci. Eng. B **212**, 7 (2016).

[40] See Supplemental Material at http://link.aps.org/supplemental/10.1103/PhysRevB.94.241110 for details about the experimental and theoretical methods, complementary raw data, and a 3D mapping of $SrVO_3$ electronic structure.

[41] Y. Muraoka, H. Nagao, S. Katayama, T. Wakita, M. Hirai, T. Yokoya, H. Kumigashira, and M. Oshima, Persistent insulator-to-metal transition of a VO_2 thin film induced by soft X-ray irradiation, Jpn. J. Appl. Phys. **53**, 05FB09 (2014).

[42] T. C. Rödel, C. Bareille, F. Fortuna, C. Baumier, F. Bertran, P. Le Fèvre, M. Gabay, O. Hijano Cubelos, M. J. Rozenberg, T. Maroutian, P. Lecoeur, and A. F. Santander-Syro, Orientational Tuning of the Fermi Sea of Confined Electrons at the $SrTiO_3$(110) and (111) Surfaces, Phys. Rev. Appl. **1**, 051002 (2014).

[43] J. Shen, H. Lee, R. Valentí, and H. O. Jeschke, *Ab initio* study of the two-dimensional metallic state at the surface of $SrTiO_3$: Importance of oxygen vacancies, Phys. Rev. B **86**, 195119 (2012).

[44] N. C. Plumb, M. Salluzzo, E. Razzoli, M. Månsson, M. Falub, J. Krempasky, C. E. Matt, J. Chang, M. Schulte, J. Braun, H. Ebert, J. Minár, B. Delley, K.-J. Zhou, T. Schmitt, M. Shi, J. Mesot, L. Patthey, and M. Radović, Mixed Dimensionality of Confined Conducting Electrons in the Surface Region of $SrTiO_3$, Phys. Rev. Lett. **113**, 086801 (2014).

[45] M. Casula, Ph. Werner, L. Vaugier, F. Aryasetiawan, T. Miyake, A. J. Millis, and S. Biermann, Low-Energy Models for Correlated Materials: Bandwidth Renormalization from Coulombic Screening, Phys. Rev. Lett. **109**, 126408 (2012).